Journal of Biomedical Optics

BiomedicalOptics.SPIEDigitalLibrary.org

Aberration correction during real time *in vivo* imaging of bone marrow with sensorless adaptive optics confocal microscope

Zhibin Wang
Dan Wei
Ling Wei
Yi He
Guohua Shi
Xunbin Wei
Yudong Zhang

SPIE.

Aberration correction during real time *in vivo* imaging of bone marrow with sensorless adaptive optics confocal microscope

Zhibin Wang,[a,b,c] Dan Wei,[d] Ling Wei,[a,b] Yi He,[a,b] Guohua Shi,[a,b,*] Xunbin Wei,[d] and Yudong Zhang[a,b]
[a]Chinese Academy of Sciences, The Key Laboratory on Adaptive Optics, Chengdu 610209, China
[b]Chinese Academy of Sciences, Institute of Optics and Electronics, The Laboratory on Adaptive Optics, Chengdu 610209, China
[c]University of Chinese Academy of Sciences, Beijing 100039, China
[d]Shanghai Jiao Tong University, School of Biomedical Engineering and Med-X Research Institute, 1954 Huashan Road, Shanghai 200030, China

Abstract. We have demonstrated adaptive correction of specimen-induced aberration during *in vivo* imaging of mouse bone marrow vasculature with confocal fluorescence microscopy. Adaptive optics system was completed with wavefront sensorless correction scheme based on stochastic parallel gradient descent algorithm. Using image sharpness as the optimization metric, aberration correction was performed based upon Zernike polynomial modes. The experimental results revealed the improved signal and resolution leading to a substantially enhanced image contrast with aberration correction. The image quality of vessels at 38- and 75-μm depth increased three times and two times, respectively. The corrections allowed us to detect clearer bone marrow vasculature structures at greater contrast and improve the signal-to-noise ratio. © *2014 Society of Photo-Optical Instrumentation Engineers (SPIE)* [DOI: 10.1117/1.JBO.19.8.086009]

Keywords: adaptive optics; in vivo imaging; mouse bone marrow; fluorescence; aberration correct.

Paper 140216R received Apr. 4, 2014; revised manuscript received Jul. 10, 2014; accepted for publication Jul. 11, 2014; published online Aug. 12, 2014.

1 Introduction

In vivo visualizing bone marrow has been a major attraction for biological research, especially stem cell research,[1,2] because studying biological systems as they evolve in their natural and physiological state could provide more relevant information than that in an *in vitro* environment. However, it is still big challenge for confocal fluorescence microscopy, which is widely used in biological research, to achieve optimal and diffraction-limited resolution *in vivo* imaging, especially in deep tissue.

Because biological samples are intrinsically turbid mediums (i.e., proteins, nuclear acids, and lipids) with optical properties characterized by strong multiple scattering and heterogeneity in its refractive index, and refractive mismatching between immersion media and biological samples[3] they induce optical aberrations resulting in an enlarged focal spot within the sample and a concomitant deterioration of signal and resolution.[4,5] Therefore, the resolution and contrast of confocal microscopy is compromised *in vivo*. To observe clear bone marrow structure *in vivo*, correction of aberrations induced by heterogeneity in refractive indexes is necessary.

The aberrations could be compensated by adaptive optics (AO) technique, which has been widely used in astronomy and vision science. The typical AO systems employ a sensor to measure wavefront aberration in the image-path of the optical system and correct the aberration in a feedback loop. However, these methods require a point-like reference source, such as the guide star used in astronomical systems. In vision science, AO systems found their guide-star from the stable reflection of the retina, which is a somewhat translucent tissue. Currently, AO technology has been combined with confocal scanning laser ophthalmoscope[6] and optical coherence tomography[7] to image living human retina at the single cell level.[5] They have been the basic tools in ophthalmology research.

However, in the field of microscopy, the situation is more complicated since the three-dimensional (3-D) structure of the specimen means that the reference source is generally far from point-like.[8] In fact, the wavefront sensor would receive a multitude of wavefronts emitting from different parts of the specimen. Currently, several groups have conducted research on wavefront correction related to single-photon or multiphoton scanning microscopy[8–12] with different AO correction methods. Fluorescent protein or fluorescent beads have been used as the guide star to measure aberration of tissue. Live imaging of *Drosophila* embryos was also introduced by Tao et al.[10] However, it is not always feasible to find appropriate fluorescent protein in different samples at different depths. Therefore, most of the adaptive microscope systems so far have used indirect methods for aberration measurement.[8] Wavefront sensorless AO systems operate by sequentially modulating the AO corrector and maximizing a feedback signal according to particular optimization algorithms. The modal wavefront sensor approach proposed by Booth et al.[13] sequentially measured an image quality metric with a group of setting trial aberrations. The method was investigated in detail in Ref. 14 and works well with small aberrations.[11] Model-free search methods contain stochastic, local, or global search methods,[15] such as genetic algorithm, hill-climbing algorithm, and simulated annealing algorithm. Other approaches used a wavefront measurement based on sequential measurements of the wavefront error in each segment of the aperture.[9]

*Address all correspondence to: Guohua Shi, E-mail: ioe_eye@126.com

Due to the flow characteristics of blood *in vivo* in the bone marrow vasculature, guide star methods are not suitable because it is not easy to fix the fluorescent guide star in vessels. Therefore, to achieve a stable and accurate wavefront correction for mouse bone marrow *in vivo*, we chose a sensorless AO scheme and introduced stochastic parallel gradient descent (SPGD),[16] which has been used in two-photon microscopy, as the wavefront optimization algorithm.[17] The SPGD proposed by Vorontsov has been used in other areas of AO and has been verified to be the fastest search method. Here, we demonstrate an AO confocal fluorescence microscope with SPGD optimization algorithm. A deformable mirror (DM) was used as wavefront corrector to compensate system- or specimen-included aberration. *In vivo* imaging experiment of mouse bone marrow vasculature was accomplished. The results have demonstrated that the aberration correction with the SPGD algorithm has improved the image quality and fluorescence signals.

2 Materials and Method

2.1 *Experimental Setup*

Figure 1 shows the experimental configuration used for AO aberration correction and *in vivo* fluorescence imaging. The beam light emitted from a 638-nm diode (LD) with output power ~30 mW was collimated. The expanded beam was imaged onto a DM with 37 actuators. Then, two scanning mirrors were used to scan the laser in the X and Y directions (the objective axis being the Z direction). To keep the phase correction stationary during beam scanning, the DM was conjugated to the X scanner and the X and Y scanners were conjugated to each other, which was then conjugated to the back pupil plane of the objective. All the optical conjugation was achieved by custom-designed spherical mirrors. The fluorescence emission was collected by an objective lens (Olympus UA, water immersion, 20×, NA = 0.5, Japan). The working distance of the objective is 3.5 mm. A band-pass filter (Semrock, FF01-670/30 nm, Rochester, New York) was placed before the photomultiplier tubes (PMT, Hamamatsu, H7422-20, Japan) to filter illumination light. The pinhole used in this microscope was 50 μm. Finally, the fluorescence from the specimen was detected by PMT. Specimen scanning in the axial Z direction was enabled by a motorized translation stage. The theoretical lateral resolution and axial resolution are 0.55 and 3.8 μm, respectively. A Hartmann wavefront sensor was used to measure system aberration and for calibration of the Zernike basis mode.[13] The imaging speed of the microscope was 30 Hz.

2.2 *AO Optimization Algorithm*

The SPGD algorithm maximizes or minimizes a selected metric value of the imaging system in an iterative control loop. The control loop for AO includes temporarily changing the DM shape by applying perturbations on its independent control inputs, assessing the effect of these perturbations on the metric, estimating a metric gradient with respect to the control input perturbations, and finally updating the mirror shape.

Zernike polynomials, which are the most commonly used modes in microscopy and which have certain well-known advantages[18] compared with other modal representations,[19] were chosen to be control basis of the SPGD algorithm. The DM shape was changed by applying perturbations on the Zernike polynomial coefficients, and it proved to have a faster convergence speed compared to perturbing each actuator in the SPGD algorithm.[17]

The aberration in pupil could be expanded as

$$\Phi(u, v) = \sum a_i Z_i(u, v), \tag{1}$$

where $Z_i(u, v)$ is the i'th Zernike polynomials with coefficient a_i.

The SPGD algorithm could be expressed as

$$a_i^{n+1} = a_i^n + k\delta_i^n(J^{n+} - J^{n-}), \tag{2}$$

where δ_i^n is the randomized perturbation applied for the i'th control channel, coefficient of i'th Zernike polynomial, in a direction randomly signed; J^{n+} is the metric when randomized perturbations $(\delta_1^n, \delta_2^n, \ldots, \delta_i^n, \delta_{i+1}^n \ldots)$ are applied for all control channels; and J^{n-} is the metric when the control channels are perturbed in the opposite direction. In the main loop, the perturbations are computed using a superposition of Zernike modes. Then, a predefined number of images of the specimen are recorded and analyzed. The metric values are stored for

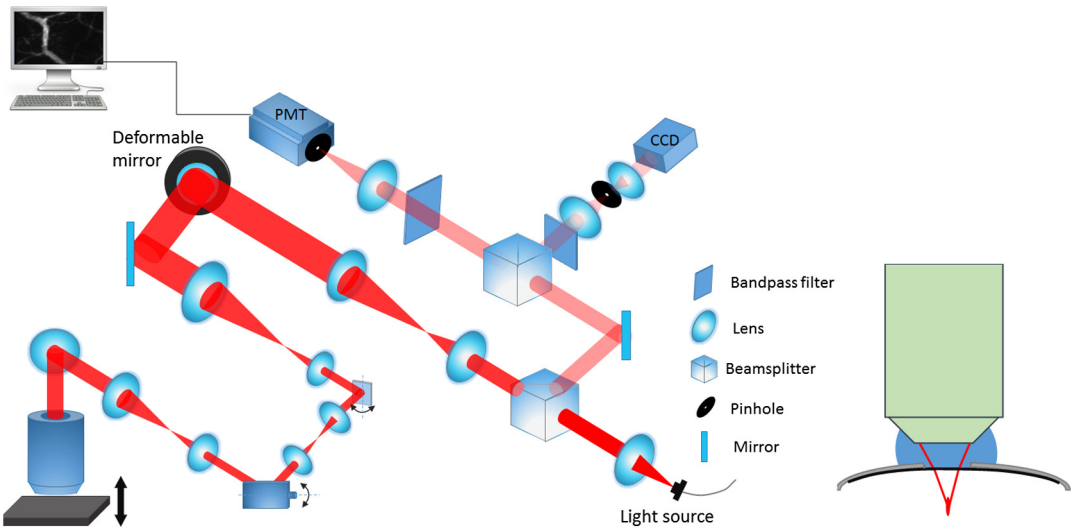

Fig. 1 Schematic diagram of the adaptive optical confocal fluorescence microscopy.

every image. Then, the Zernike coefficients are taken as the new starting point for further optimization.

In this paper, image sharpness,[20] robust for the design of a sample-independent aberration correction scheme, was chosen as the metric of image quality. The first 15 Zernike polynomials[8] except the first three polynomials are used for aberration correction in this paper. Tip, tilt, and defocus components are removed from the basis modes because they do not affect image quality but only cause an offset of focus position in three directions.

2.3 *Specimen Preparation*

For *in vivo* imaging, BALB/c-nu mice were deeply anesthetized with pentobarbital (Sagital, 80 mg/kg i.p.). Then, a small incision was made in the scalp to expose the underlying frontoparietal skull surface. A plastic ring was inserted in the incision to spread the skin and to allow application of sterile physiologic saline solution to prevent drying of the tissue. For bone marrow vessel imaging, the fluorescent lipophilic tracers DiD (molecular probes) were injected into the tail vein. The bone marrow vasculature of the skull was then imaged using the custom-built fluorescence confocal microscope while the mice were

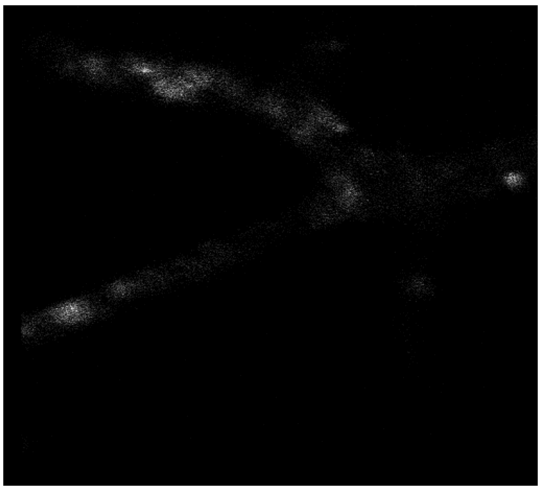

Video 1 Video of the bone marrow vasculature at 38-μm depth during aberration correction (MOV, 7.31 MB) [URL: http://dx.doi.org/10.1117/1.JBO.19.8.086009.1].

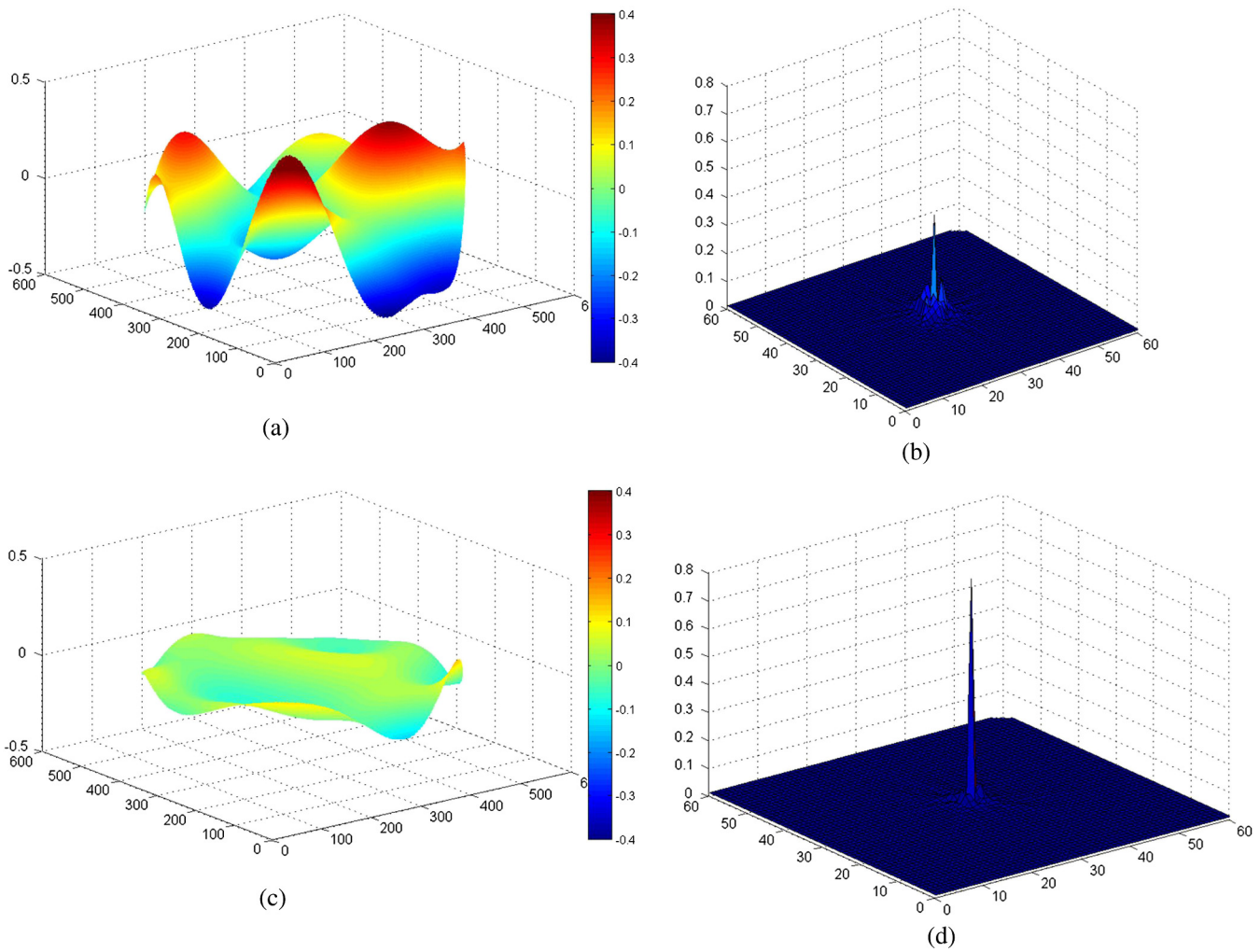

Fig. 2 (a) Wavefront of system aberration measured by Hartmann sensor. (b) Point spread function (PSF) of system before system-induced aberration correction. (c) Wavefront of residual aberration measured after correction of system aberration. (d) PSF of system after aberration correction.

under anesthesia on a warmed microscope stage. High-resolution images were obtained through the intact mouse skull at depths of up to hundreds of microns from the surface of the skull using a water immersion objective lens.

3 Results

First, a Hartmann wavefront sensor was used to measure system aberration using a fluorescence bead attached to the glass slide as the guide star and the system aberration was compensated before imaging experiment *in vivo*. Root mean square (RMS) of system aberration was 0.142 μm. After aberration correction, RMS went down to 0.079 μm. The corresponding point spread functions of microscopy before and after AO correction are also shown in Fig. 2.

Using molecular probes injected into mouse vein, fluorescence images of a bone marrow vasculature 38 μm below the surface of the skull was obtained, and aberration correction was accomplished as shown in Video 1.

Lateral images of the vasculature before and after AO correction are shown in Fig. 3(a). As seen from this figure, in addition to a great enhancement of the fluorescence signal, the details of the vessel are more abundant, since the aberration correction could improve resolution of the microscope. A sharper image of one cell in the vasculature, shown in magnified image of Fig. 3(a), was achieved.

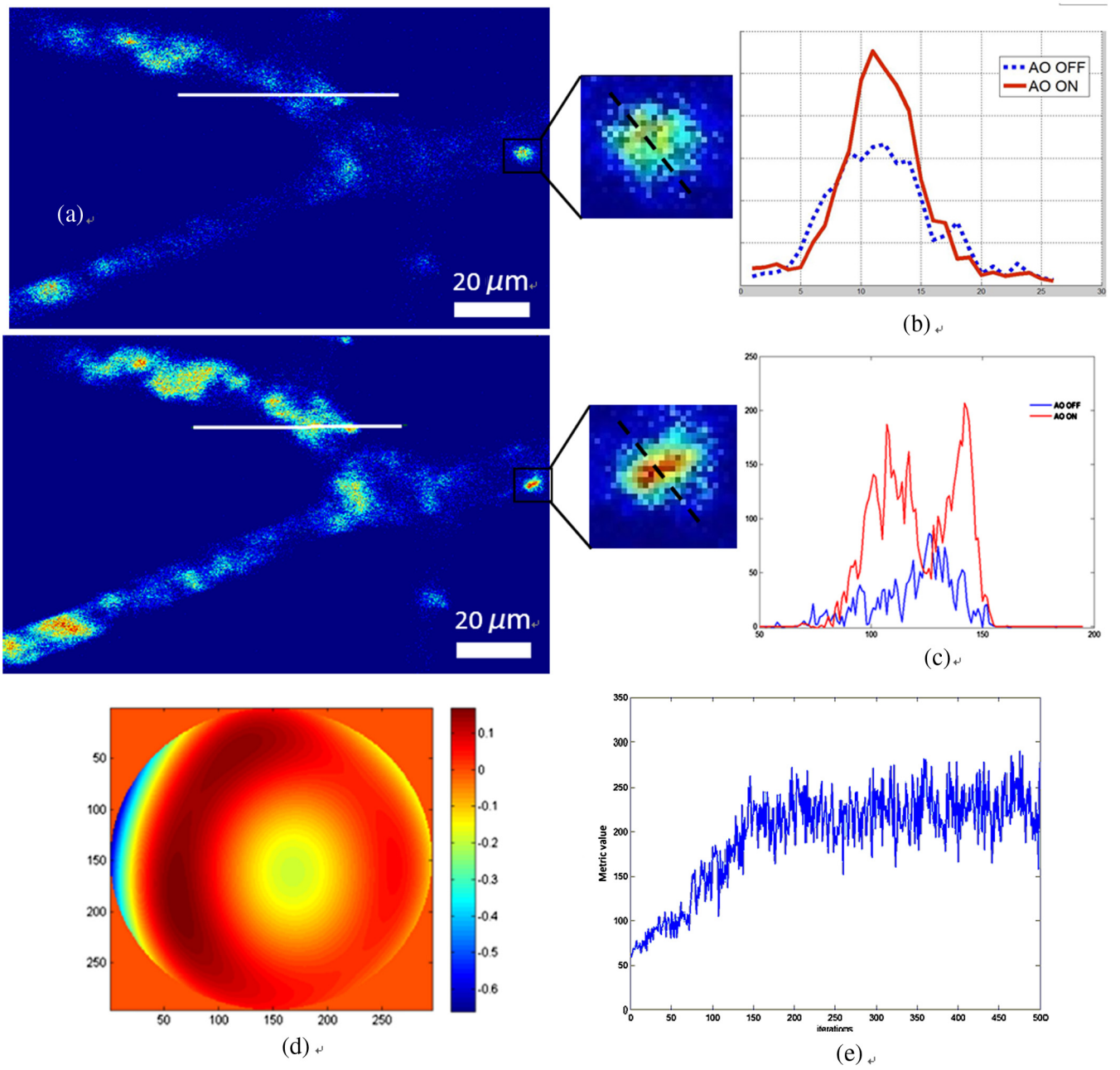

Fig. 3 (a) Lateral fluorescence bone marrow vasculature images 38 μm below the skull surface before and after aberration correction. (b) Fluorescence signal profiles along the black dot line in (a). (c) Signal profiles along the white line in (a). (d) The final corrective wavefront of deformable mirror (DM). (e) Metric value of images during aberration correction process.

The signal profile along the white line in Fig. 2(a), shown in Fig. 3(c), reveals that the improved signal and resolution result in substantially enhanced contrast. The metric values of images during the aberration correction process are shown in Fig. 3(e). After 150 iterations, the metric value of images increased threefold with the same excitation power. It takes about 5 s to complete the correction for our microscope. The compensation profile of the DM is shown in Fig. 3(d).

It is a common observation that image resolution and contrast degrade with imaging depth. In Fig. 4, we summarize the fluorescence images of the vasculature at depths down to 75 μm without AO correction and with AO correction. The video during aberration correction is shown in Video 2. We also present the signal profile along the dotted line in Fig. 4(a), which reveals the improved signal and resolution results with enhanced contrast, therefore, more vasculature detail can be defined after correction.

The metric value of the image after AO correction, shown in Fig. 4(d), increased nearly twofold with the same excitation power. It takes about 150 to 200 iterations to complete the correction. It also reveals that the closed-loop stability decreases, because the index-mismatch aberration increases with image

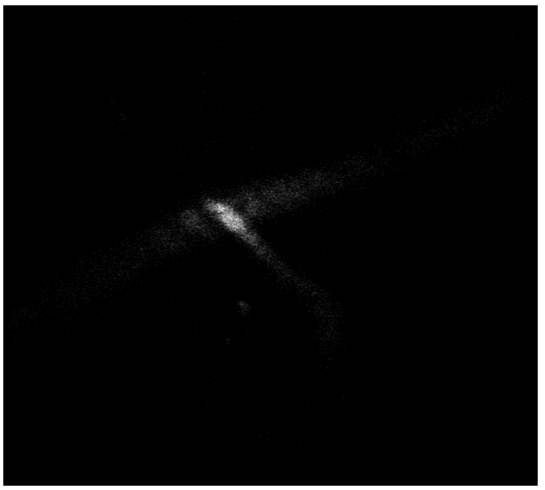

Video 2 Video of the bone marrow vasculature at 75-μm depth during aberration correction (MOV, 3.50 MB) [URL: http://dx.doi.org/10.1117/1.JBO.19.8.086009.2].

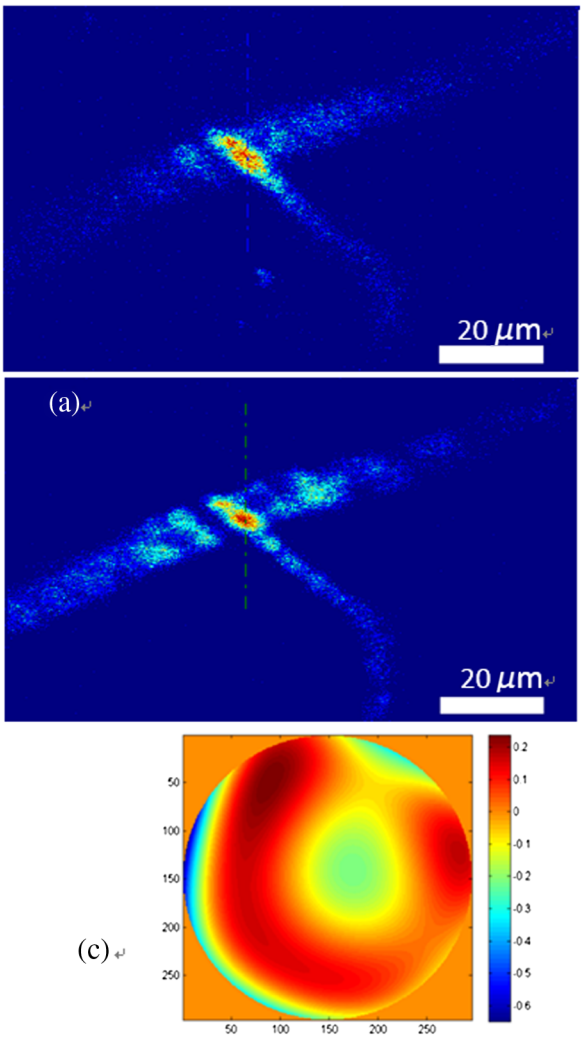

Fig. 4 (a) Lateral fluorescence bone marrow vasculature image 75 μm below the skull surface before and after adaptive optics correction. (b) Fluorescence signal profiles along the dot line in Fig. 2(a). (c) The final corrective wavefront of DM. (d) Metric value of images during aberration correction process.

depth and perturbations during SPGD iterative process may go beyond the capability of the DM to compensate. The compensation profile of the DM is shown in Fig. 4(c).

The aberration corrected images obtained with the microscope show enhanced contrast and improvement of fluorescence intensity. The AO could be widely beneficial in confocal microscopes that often suffer from the detrimental effects of system- and specimen-induced aberrations, especially for *in vivo* imaging.

4 Discussion and Conclusion

In vivo bone marrow vasculature imaging has played an important role in research regarding the dynamic interactions between tumor/stem cells and the bone marrow microenvironment. We have demonstrated confocal fluorescence microscopy with a sensorless AO system which could be used for *in vivo* imaging of mouse bone marrow. The results show improved imaging depth and imaging resolution. With aberration correction, finer bone marrow cavity structure information and more accurate locations of cells could be observed.

The custom built confocal fluorescence microscope could perform real-time imaging at the video level, which is ideally suited for *in vivo* imaging and long-term observation of vascular cells within the bone marrow.

Because of the flow characteristics of blood, guide star methods are not suitable because it is not convenient to fix injected fluorescent beads or find fluorescent proteins in vessels *in vivo*. Therefore, a wavefront sensorless scheme was chosen in the microscopy. Compared to conventional AO using direct wavefront sensing which needs a guide star and wavefront sensor, such as the Hartmann sensor, to measure the aberration of the imaging-path from the guide star, sensorless AO has a simpler system architecture and can non-invasively correct aberrations for different depths of biological tissue, which is very important in the field of microscopy.

The aberration magnitudes of bone marrow during *in vivo* imagine have significant variations at different imaging depths. Therefore, the AO method should be adaptive to correct different magnitudes of aberrations. An optimization algorithm based on a random search was selected because of its advantages of better convergence robustness for aberrations of various magnitudes. Compared to the modal sensor algorithm, it is simple and does not require a system calibration process.[21] The modal sensor needs a different control basis for different magnitudes' aberrations[22,23] and also requires a complex system calibration process.[21] Correction speed also has important significance for fluorescence imaging because of the photo bleaching issue for fluorescent dyes. Considering the range of the algorithm application and correction speed, we choose the SPGD algorithm, which has robust convergence characteristics for different aberrations and can complete the aberration correction in seconds in a confocal fluorescence microscope, which is first time this has done to the best of our knowledge.

The experiment of *in vivo* mouse bone marrow imaging was completed. Fluorescence images of blood vessels at different depths are obtained and image contrast has been significantly improved after correction. For the blood vessel at the depth of 38 μm, the convergence process was relatively stable and more blood cell morphology can clearly be observed after correction. For the blood vessel at the depth of 75 μm, enhancement of the fluorescence intensity after correction was also observed, but the stability of the convergence process decreased. The main reason is that the fitting ability of the DM is limited by the drive stroke volume; therefore, some drives were saturated with deeper imaging position. In addition, the lower resolution of the image of a deeper blood vessel after correction was observed, mainly due to more severe scattering.[24] The results prove that the image-based wavefront sensorless AO with the SPGD algorithm could meet the requirements of aberration correction for *in vivo* imaging in real-time confocal microscopy.

For the optimization of the first 15 Zernike modes, typically 100 to 200 images are necessary to achieve good correction results. It takes 5 to 7 s to accomplish aberration correction, which is not conducive in the cases with more stringent time requirements. The convergence time is mainly limited by the imaging speed of the microscope and the convergence rate of the SPGD algorithm. An improved SPGD algorithm or combining it with other optimization algorithms such as the modal algorithm may be a potential solution to accelerate the process of aberration correction. This will be the next focus of our future work.

To conclude, by incorporating an SPGD-based AO in a confocal fluorescence microscope, we demonstrated that the correct use of AO reduces specimen-induced aberrations *in vivo* in the mouse skull marrow. The fluorescence images with aberration correction show enhanced contrast and improvement of fluorescence intensity. Therefore, AO would play an important role in the application of many physiological imaging techniques *in vivo*. While the confocal fluorescence microscopy could perform real-time imaging of blood vessels. Not only can the 3-D structure be observed, but the migration of blood cells or other observations of immune cells in the blood vessels can also be observed. It would be the ideal tool for study of vascular dynamics in future.

Acknowledgments

This work is supported by the National Major Scientific Equipment program (Grant No. 2012YQ120080), the National Science Foundation of China (Grant No. 61108082), the Sichuan Youth Science and Technology Foundation (Grant No. 2013JQ0028), and the West Light Foundation of the Chinese Academy of Sciences. The authors would like to thank Hao Li and Jing Lu for many helpful discussions regarding this project.

References

1. D. A. Sipkins et al., "In vivo imaging of specialized bone marrow endothelial microdomains for tumour engraftment," *Nature* **435**(7044), 969–973 (2005).
2. C. L. Celso, J. W. Wu, and C. P. Lin, "In vivo imaging of hematopoietic stem cells and their microenvironment," *J. Biophotonics* **2**(11), 619–631 (2009).
3. P. Török, S. Hewlett, and P. Varga, "The role of specimen-induced spherical aberration in confocal microscopy," *J. Microsc.* **188**(2), 158–172 (1997).
4. M. Schwertner, M. Booth, and T. Wilson, "Characterizing specimen induced aberrations for high NA adaptive optical microscopy," *Opt. Express* **12**(26), 6540–6552 (2004).
5. M. Booth, M. Neil, and T. Wilson, "Aberration correction for confocal imaging in refractive-index mismatched media," *J. Microsc.* **192**(2), 90–98 (1998).
6. J. Lu et al., "Retina imaging in vivo with the adaptive optics confocal scanning laser ophthalmoscope," *Proc. SPIE* **7519**, 75191 (2009).
7. B. Hermann et al., "Adaptive-optics ultrahigh-resolution optical coherence tomography," *Opt. Lett.* **29**(18), 2142–2144 (2004).

8. M. J. Booth et al., "Adaptive aberration correction in a confocal microscope," *Proc. Natl. Acad. Sci.U.S.A.* **99**(9), 5788–5792 (2002).
9. N. Ji, T. R. Satoa, and E. Betziga, "Characterization and adaptive optical correction of aberrations during in vivo imaging in the mouse cortex," *Proc. Natl. Acad. Sci.U. S. A.* **109**(1), 22–27 (2012).
10. X. Tao, J. Crest, and S. Kotadia, "Live imaging using adaptive optics with fluorescent protein guide-stars," *Opt. Express* **20**(14), 15969–15982 (2012).
11. D. Débarre et al., "Image-based adaptive optics for two-photon microscopy," *Opt. Lett.* **34**(16), 2495–2497 (2009).
12. L. Sherman et al., "Adaptive correction of depth-induced aberrations in multiphoton scanning microscopy using a deformable mirror," *J. Microsc.* **206**(1), 65–71 (2002).
13. M. J. Booth, M. A. A. Neil, and T. Wilson, "New modal wave-front sensor: application to adaptive confocal fluorescence microscopy and two-photon excitation fluorescence microscopy," *J. Opt. Soc. Am. A* **19**(10), 2112–2120 (2002).
14. A. Facomprez, E. Beaurepaire, and D. Debarre, "Accuracy of correction in modal sensorless adaptive optics," *Opt. Express* **20**(3), 2598–2612 (2012).
15. W. Lubeigt et al., "Search-based active optic systems for aberration correction in time-independent applications," *Appl. Opt.* **49**(3), 307–314 (2010).
16. M. A. Vorontsov et al., "Adaptive optics based on analog parallel stochastic optimization: analysis and experimental demonstration," *J. Opt. Soc. Am. A* **17**(8), 307–314 (2000).
17. Y. Zhou, T. Bifano, and C. Lin, "Adaptive optics two photon scanning laser fluorescence microscopy," *Proc. SPIE* **7931**, 79310H (2011).
18. D. Malacara, *Optical Shop Testing*, 7th ed., Wiley-Interscience, Hoboken, NJ (2007).
19. J. Braat, "Polynomial expansion of severely aberrated wavefronts," *J. Opt. Soc. Am. A* **4**(4), 643–650 (1987).
20. M. A. Vorontsov et al., "Image quality criteria for an adaptive imaging system based on statistical analysis of the speckle field," *J. Opt. Soc. Am. A* **13**(7), 1456–1466 (1996).
21. A. Thayil and M. J. Booth, "Self calibration of sensorless adaptive optical microscopes," *J. Eur. Opt. Soc.* **6**, 11045 (2011).
22. M. J. Booth, "Wavefront sensorless adaptive optics for large aberrations," *Opt. Lett.* **32**(1), 5–7 (2007).
23. M. J. Booth, "Wave front sensor-less adaptive optics: a model-based approach using sphere packings," *Opt. Express* **14**(4), 1339–1352 (2006).
24. E. Chaigneau et al., "Impact of wavefront distortion and scattering on 2-photon microscopy in mammalian brain tissue," *Opt. Express* **19**(23), 22755–22774 (2011).

Zhibin Wang is a PhD candidate at the Key Laboratory on Adaptive Optics, Institute of Optics and Electronics, Chinese Academy of Sciences. He received his BS degree in automation from the University of Science and Technology of China in 2010. His current research interests include biomedical imaging, adaptive optics, and optoelectronic systems.

Biographies of the other authors are not available.